Separating isotopic impacts of karst and in-cave processes from climate variability using an integrated speleothem isotope-enabled forward model

Pauline C. Treble[1,3], Mukhlis Mah[2, 3], Alan Griffiths[1], Andy Baker[2, 3], Michael Deininger[4], Bryce F. J. Kelly[2, 3], Denis Scholz[4], Stuart I. Hankin[1]

[1]ANSTO, Lucas Heights, NSW 2234, Australia

[2]Connected Waters Initiative Research Centre, UNSW Sydney, Sydney 2052, Australia

[3]School of Biological, Earth and Environmental Sciences, UNSW Sydney, Sydney 2052, Australia

[4]Institute for Geosciences, University of Mainz, Johann-Joachim-Becher-Weg 21, 55128 Mainz, Germany

Correspondence to: Pauline Treble (pauline.treble@ansto.gov.au)

Abstract. Speleothem $\delta^{18}O$ values are commonly used to infer past climate variability. However, both non-linear karst hydrological processes and in-cave disequilibrium isotope fractionation are recognised and hinder the interpretation of $\delta^{18}O$ values. In recent years, proxy system models (PSMs) have emerged to quantitatively assess the confounding effects of these processes. This study presents the first integrated stalagmite $\delta^{18}O$ PSM (Karstolution) by coupling an existing karst hydrology with an in-cave fractionation PSM. The new modelling framework not only couples the two models, but also includes diffuse flow modelling, coupling of drip rate with infiltration, linking of surface with cave temperature, and incorporates cave seasonality effects. We test Karstolution using a cave monitoring dataset from Golgotha Cave, SW Australia. The predictive capacity of the model is assessed by comparing the output to stalagmite $\delta^{18}O$ values. By comparing with observed stalagmite $\delta^{18}O$ values, this study is also the first to quantify in-cave disequilibrium both kinetic isotopic fractionation in a speleothem and informs the conclusion that hydroclimatic processes contributes more to the variability of stalagmite $\delta^{18}O$ values at Golgotha Cave than does in-cave processes. This is further supported via a sensitivity analysis performed by simulating the impacts of a wider range of cave temperature, ventilation, drip interval and pCO_2 values than measured.

Keywords: proxy system model, speleothem, ISOLUTION, karst hydrology, oxygen isotopes

1 Introduction

Speleothems provide valuable paleoclimatic information due to their long time spans (10^2 -10^4 years), precise chronology, high resolution (sub-decadal to sub-annual depending on growth rate), and relatively widespread distribution [*McDermott*, 2004]. The interpretation of speleothem $\delta^{18}O$ values is still difficult due to the non-linearity of karst hydrology and in-cave isotopic fractionation (see [Hartmann and Baker, 2017]).

Despite the common assumption that rainfall and cave dripwater $\delta^{18}O$ values have a linear relationship, cave monitoring has revealed potential non-linear processes associated with variable infiltration of recharge, mixing of various water stores, and non-linear water movement (e.g. [*Ayalon et al.*, 1998; *Baker and Brunsdon*, 2003; *Fairchild et al.*, 2006; *Mischel et al.*, 2015]. This can be further influenced by: accentuation of high magnitude precipitation [*Pape et al.*, 2010], mixing of different types of flow (e.g. fracture and diffuse flow), and soil and epikarst evaporation [*Cuthbert et al.*, 2014a].

Deposition of speleothem calcite under conditions of isotopic equilibrium implies isotopic equilibrium between $CaCO_3$, HCO_3^- and H_2O, such that the precipitated calcite is in isotopic equilibrium with the water [*Hendy*, 1971]. However, many in-cave processes may prevent equilibrium isotopic fractionation: (i) low relative humidity and in-cave air movement allow evaporative fractionation of dripwater $\delta^{18}O$ values [*Deininger et al.*, 2012]; (ii) high supersaturation of the dripwater with respect to calcite (related to both cave and soil pCO_2) results in rapid precipitation after degassing of CO_2, which may disturb the isotope equilibrium between $CaCO_3$, HCO_3^- and H_2O [*Deininger et al.*, 2012; *Mickler et al.*, 2006; Scholz et al., 2009]; (iii) the time between two subsequent drips may affect the degree of isotope disequilibrium [*Deininger et al.*, 2012; *Frisia et al.*, 2011; *Kaufmann*, 2003; *Mühlinghaus et al.*, 2007; *Mühlinghaus et al.*, 2009; *Riechelmann et al., 2013*].

To advance our capacity to interpret the climatic record in speleothems, study sites are carefully chosen, and monitoring of cave conditions, dripwater, and hydrology are established (e.g. [*Baker et al.*, 2014; *Baldini et al.*, 2012; Duan et al., 2016; *Frisia et al.*, 2011; *Markowska et al.*, 2015; Spötl *et al.*, 2005]). However, quantification of the aforementioned processes is difficult, with issues outlined with respect to the 'Hendy Test' [*Dorale and Liu*, 2009] and linear regression climate calibrations [*Baker and Bradley*, 2010]. Replication from multiple stalagmites [*Stoll et al.*, 2015], clumped isotope thermometry (Δ47; [*Affek et al.*, 2008] and analysis of fluid inclusions [*Kluge et al.*, 2008] have been proposed to demonstrate oxygen isotope equilibrium between water and speleothem calcite, but these may be difficult to apply in practice.

To provide insights on the primary drivers of speleothem $\delta^{18}O$ variability, Proxy System Models (PSMs) have emerged, using climatic inputs and numerical representation of the processes for forward modelling of the proxies [*Evans et al.*, 2013]. These models allow quantification of sensitivity to various processes affecting proxy interpretation [*Wong and Breecker*, 2015]. The quantitative approach of PSMs also facilitates simulations of 'what-if' climate scenarios to be compared against proxy data (e.g. [*Baker et al.*, 2012]), as well as assisting with constraining climate models, especially in the emergent field of paleoclimate data assimilation (e.g. [*Dee et al.*, 2016].

Hence, a number of karst and speleothem PSMs have been developed (Table 1). However, the majority of the stalagmite $\delta^{18}O$ PSMs focus either on karst processes or in-cave processes and adopt a simplified representation of the other part of the system. Of these, KarstFor [*Bradley et al.*, 2010] and ISOLUTION [*Deininger et al.*, 2012], represent the most advanced treatment of the processes affecting $\delta^{18}O$ values in the karst and cave, respectively.

Using a lumped parameter approach to model the complexities of karst hydrogeology, KarstFor was first presented in Bradley et al. (2010) and subsequently enhanced with multiple adaptations (e.g. [*Baker and Bradley*, 2010; *Baker et al.*, 2013; *Treble et al.*, 2013]. The initial iterations of KarstFor consisted of climatic inputs (Table 2) and a monthly time-step for reservoirs representing the soil, epikarst and vadose zone. This accounted for evaporative oxygen isotope fractionation in the soil store and represented water-balance, mixing, overflow and underflow movement. The approach was highly parameterised, thus requiring constraints by site-specific knowledge, and assumed in-cave equilibrium isotope fractionation (using the [*Kim and O'Neil*, 1997] fractionation factor between water and calcite).

Table 1: Summary of existing stalagmite and karst based forward models (PSMs) excluding catchment scale karst models.

Model name	Description	Published
In-Cave Processes (No Karst Processes)		
	Model of stalagmite growth and $\delta^{13}C$ values on the stalagmite surface solution.	[*Romanov et al.*, 2008a; b]
ISOLUTION	Model of in-cave evaporation and isotope fractionation processes affecting stalagmite growth, $\delta^{13}C$ and $\delta^{18}O$ values.	[*Deininger et al.*, 2012; *Mühlinghaus et al.*, 2009; *Scholz et al.*, 2009]
	Stalagmite growth model based on in-cave conditions (drip saturation, pCO_2 and cave temperature) and climatic inputs.	[*Kaufmann, 2003; Mühlinghaus et al., 2007; Baker et al.*, 2014]
I-STAL	Model of dripwater Mg, Sr and Ba from drip rate and drip saturation with respect to calcite; also represents prior calcite precipitation and dripwater chemistry.	[*Stoll et al.*, 2012]
	Model of the temporal isotopic ($\delta^{18}O$ and $\delta^{13}C$) evolution of DIC in a thin film precipitating calcite.	[*Dreybrodt and Romanov, 2016*]
Soil and In-Cave Processes (No Karst Processes)		
ODSM	Model of stalagmite $\delta^{18}O$ values from climatic input, soil mixing and vegetation effects. Soil water was modelled straight to in-cave and temperature dependent fractionation applied.	[*Wackerbarth*, 2012; *Wackerbarth et al.*, 2010; *Wackerbarth et al.*, 2012]
	Model of $\delta^{13}C$ and $\delta^{18}O$ values in soil (against soil pCO_2) and in-cave isotope fractionation processes.	[*Dreybrodt and Scholz*, 2011]
CaveCalc	PHREEQC-based model of soil, bedrock and in-cave processes including isotopes and trace elements	Owen et al. (2018)
Karst Processes (No In-Cave Processes)		
	Climatically fed single reservoir model with fracture flow for high magnitude rainfall and diffuse flow for low magnitude rainfall.	[*Baker et al.*, 2010; *Nagra et al.*, 2016]
	Two layer reservoir dripwater $\delta^{18}O$ model based on climatic input, with stores modelled as steady state.	[*Truebe et al.*, 2010]
KarstFor	Three (or four) layer reservoir model with soil evaporation, monthly water balance, overflow and underflow based on climatic input. Dripwater $\delta^{18}O$ values include temperature dependant isotope fractionation.	[*Baker and Bradley*, 2010; *Baker et al.*, 2013; *Baker et al.*, 2010; *Fairchild and Baker*, 2012; *Jex et al.*, 2013; *Treble et al.*, 2013]
	Two reservoir dripwater $\delta^{18}O$ model based on climatic input and defined residence time.	[*Moerman et al.*, 2014]
	Two layer reservoir model with daily water balance, mixing of $\delta^{18}O$ values and epikarst evaporation to model dripwater $\delta^{18}O$ values.	[*Cuthbert et al.*, 2014]
	Two reservoir discharge model with daily water balance.	Campbell et al., 2017
KARSTMOD	Variable reservoir model of discharge at karst springs based on climatic input.	[*Jourde et al.*, 2015]
PRYSM	Open source GCM enabled single reservoir model using a mean transit time, τ. PRYSM includes models for other climate sensors (e.g. ice cores) and incorporates the errors associated with age assignments.	[*Dee et al.*, 2015]

ISOLUTION [*Deininger et al.*, 2012] simulates speleothem $\delta^{18}O$ values in dependence of cave temperature, drip interval, cave air pCO_2, dripwater pCO_2 (an equivalent for the dripwater Ca^{2+} concentration), relative humidity and cave ventilation during speleothem growth. ISOLUTION is based on previous models describing speleothem growth and stable isotope fractionation (see [*Deininger et al.*, 2012] and [*Deininger and Scholz*, 2019] for details). By including in-cave oxygen isotope disequilibrium and evaporative fractionation effects [*Deininger et al.*, 2012], ISOLUTION is currently the most advanced model describing speleothem oxygen isotope fractionation effects.

Here we present the first stalagmite $\delta^{18}O$ PSM combining karst and in-cave processes (Karstolution). This integrated surface-to-stalagmite $\delta^{18}O$ PSM is a coupling of the KarstFor and ISOLUTION models and allows for the first time the quantification of the effects of both karst and in-cave processes. Karstolution includes the addition of diffuse flow, growth rate, modelling of in-cave seasonality and the coupling of drip infiltration and cave temperature. We present a case study of Golgotha Cave using monitoring data first presented by Treble et al. (2013) as well as data from recently deposited calcite. Based on these data, we show how the Karstolution parameters can be localised to a particular cave site and demonstrate how the model can be used to evaluate the relative effects of climatic, karst and in-cave processes. As the conceptual model of Karstolution is generic it is not limited to Golgotha Cave and can be applied to any karst setting.

2 Karstolution overview

Karstolution is a generic model that may be applied to many different karst settings, it couples KarstFor and ISOLUTION and is the first integrated surface to stalagmite $\delta^{18}O$ PSM. The model is coded in Python, with all code available on GitHub (https://github.com/swasc/karstolution). Karstolution is based on a phenomenological representation of a karst system (Fig 1; Table 2) that is not derived from fundamental laws. This has the advantage of limiting the model complexity, thus making it relatively simple to reason with, fast to execute, and easier to configure. Disadvantages include: model parameters that are not simple to relate to physical properties of the system, and limited ability to precisely reproduce the observed time series. The model is mainly suited to hypothesis testing. For example, isolating the impact of individual forcings, or varying these forcings through time. Model calibration can be treated as an iterative process, beginning with a single active flow path, followed by step-by-step introduction of more complexity.

The karst component of the model follows the KarstFor version presented in *Baker et al.* [2013], with water levels in reservoirs (Soil Store, Epikarst, KS1 and KS2) given an initial value (mm) and then recalculated (starting from the top store) at a monthly time step, via:

$$\Delta V = (\sum In - \sum Out)\,\Delta t$$

where ΔV = net change in store volume (mm) per month, *In* = input flows and *Out* = output flows (mm/month) [either: fracture flow, diffuse flow or rainfall (Fig. 1)], and Δt =1 month.

The $\delta^{18}O$ values in each store are updated with the time step based on the water balance calculations. Three stalagmite outputs, representing multiple karst configurations, are modelled as per *Baker et al.* [2013]. At each stalagmite output, the ISOLUTION model is applied to account for potential in-cave fractionation processes, using the $\delta^{18}O$ value of the input reservoir water and the cave parameters outlined in Table 2, to simulate stalagmite $\delta^{18}O$ values. For further description of the ISOLUTION model, we refer the reader to *Deininger et al.* [2012] and Deininger and Scholz (2019). Additional modelling capabilities: 1. in-cave seasonality, 2. diffuse flow, 3. the coupling of drip rate between the KarstFor and ISOLUTION models, as well as 4. stalagmite growth rate) have been added and are described below.

2.1 In-cave seasonality

The factors that may affect in-cave fractionation of $\delta^{18}O$ values can vary seasonally or at even higher frequency [*Baker et al.*, 2014; *Markowska et al.*, 2015; *Spötl et al.*, 2005; *Treble et al.*, 2015]. For example, seasonal cave ventilation can control cave air pCO_2, an important factor affecting dripwater supersaturation and, as a consequence, disequilibrium oxygen isotope fractionation, as well as leading to seasonal biases in speleothem growth and geochemistry [*Baldini et al.*, 2008; *James et al.*, 2015; *Spötl et al.*, 2005]. As continuous cave parameter time series are rarely measured, it is not practical to require this as an input series. Therefore, Karstolution allows the user to define seasonality of all factors that potentially affect in-cave oxygen isotope fractionation at their site through monthly averages of the cave parameters for each month of the year. The model additions in the next sections preserve this user-defined seasonality in its calculations.

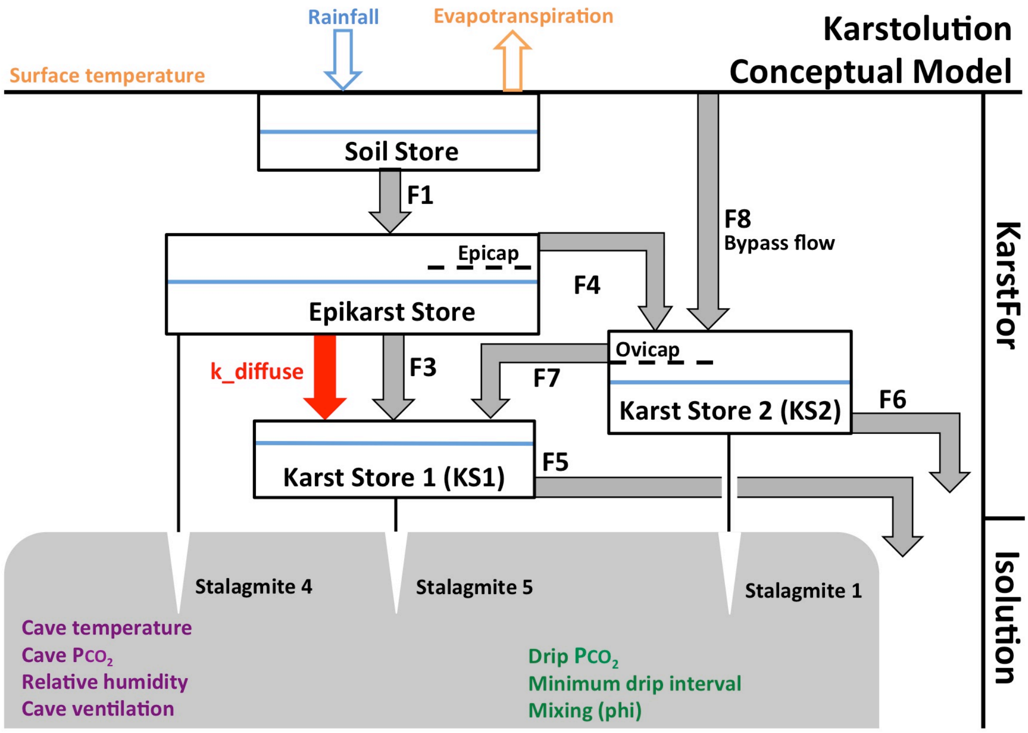

Figure 1. Conceptual figure of the Karstolution model. The boxes represent reservoirs, blue lines represent water levels, grey arrows represent fracture flow, and the red arrow represents diffuse flow. While a brief overview of the overall model is given in the main text, the details of the KarstFor and ISOLUTION models are given in Baker et al. [2013] and Deininger et al. [2012], respectively. Details of the coupling of the two models, modifications and additions are outlined in the main text. Each stalagmite output takes into account the effect of various cave parameters as described by ISOLUTION. See Table 2 for a summary of model inputs and parameters.

2.2 Dripwater coupling

The residence time of the surface water layer on the stalagmite controls the degree of the resulting isotopic disequilibrium [*Deininger et al.*, 2012; *Scholz et al.*, 2009]. As this residence time is dictated by the drip interval, which in turn is dependent on karst hydrology, modelling of the drip interval from the karst is necessary for application of ISOLUTION. We model drip-infiltration as gravity fed, with a linear response to the volume present in the karst store. Users specify the drip rate when the store is empty, q_0, and full, q_1, and the model calculates the instantaneous drip rate, q according to

$$q = (q_1 - q_0)\frac{ksize}{kstor} + q_0$$

where *ksize* is the capacity of the karst store directly supplying the drip (mm) and *kstor* is the current level of the karst store (mm; blue line in the stores shown in Fig. 1). The modelled drip interval, DI, is then

$$DI = \begin{cases} 1/q & q > 0 \\ 9001 & q \leq 0 \end{cases}.$$

This allows for a choice of q_0 and q_1 where dripping stops before the store empties completely and represents the "no drip" state with a placeholder value.

2.3 Temperature coupling

Cave temperature is a key parameter for modelling stable isotope fractionation as well as the kinetics of calcite precipitation. Previously, the KarstFor model approximated cave air temperature as surface air temperature. However, this may not be the case due to the time taken for a surface heat signal to diffuse through bedrock [*Domínguez-Villar et al.*, 2013]. Disequilibrium between surface and cave temperature may be affected by factors such as land use change, shading, fire, and rapid climate change [*Domínguez-Villar et al.*, 2015; *Nagra et al.*, 2016]. To deal with this, surface-cave temperature coupling is implemented in Karstolution with a site-specific difference between the ground surface and cave air temperature (ΔT_{S-C}). While maintaining ΔT_{S-C}, cave temperature varies using a user-defined moving average of the surface temperature (36-months in this study). A useful guide for temperature-depth penetration at different time periods is, for instance, presented in Fig. 9 of *Rau et al.* [2015].

Table 2. Compilation of selected model parameter values with notes about their implementation and configuration. All parameter names are from conceptual Figure 1. Final configuration based on Treble et al. (2013) and updated here.

Parameter	Description	Final configuration*
Soil store (mm)	Set to a small configuration with no soil evaporative fractionation as per field observations	Init: 150 Max: 500
Epikarst (mm)	Set to a small configuration with no epikarst evaporative fractionation as per field observations	Init: 30 Max: 50 Epicap: 35
KS1 (mm)	Primary karst store that receives flux from epikarst via k_diffuse and/or F3; may also receive overflow from KS2.	Init: 200 Max: 870
KS2 (mm)	Secondary karst store that fills via F4 and drains via F6 or permits modelling of switchable overflow to KS1 via F7. Magnitude of overflow is proportional to KS2/KS1 ratio.	Init: 1000 Max: 1400 Ovicap: 1150
F1 (mm/month)	Determines steady state values in soil store.	1.0
F3 (mm/month)	Flux representing fracture flow from Epikarst to KS1. Set to zero according to field observations of flow dominated by diffuse flow.	0
F4 (mm/month)	Flux from Epikarst to KS2 activated when threshold 'Epicap' is reached.	0.2
F5 (mm/month)	Drainage flux of KS1.	0.14
F7 (mm/month)	Overflow from KS2 back into KS1 once 'ovicap' is exceeded.	1.0
F6 (mm/month)	Drainage flux of KS2.	0.015
F8 (mm/month)	Bypass flow from the surface to KS2. Used to test configuration used by Treble et al. (2013) that KS2 was preferentially being recharged by rainfall events >7mm. /month, but set to zero in final configuration.	0
k_diffuse (mm/month)	Flux is via pdf function to simulate diffuse flow.	0.5
ϕ	Mixing parameter of dripwater with the water layer on the stalagmite surface	1 (based on observations of limited drip splashing)
k_eevap	Fraction of water remaining in epikarst available to evaporate	0.1 (i.e. 10% per month)
k_d18O_soil	Isotopic evaporation coefficient for soil store	‰ month^{-1} mm^{-1}
k_d18O_epi	Isotopic evaporation coefficient for epikarst store	‰ month^{-1} mm^{-1}

2.4 Diffuse flow

Diffuse flow is an important addition to the previous fracture-flow-only versions of KarstFor [*Baker and Bradley*, 2010], which would have poorly simulated sites with significant diffuse flow. Here, diffuse flow includes flow through smaller fractures as well as the matrix and mathematically, no mixing occurs along streamlines. Conversely, fracture flow is modelled as flow into reservoirs which are immediately mixed. Following from the approach of Treble et al. (2013), Karstolution uses a Weibull distribution to model diffuse flow. This was chosen because the Weibull distribution is a generalisation of the Exponential and Rayleigh distributions, and has a variable shape and skewness and hence can represent a large variety of possible transit time distributions [*Almalki and Nadarajah*, 2014]. The need to model variable flow distributions has been demonstrated for a novel D_2O irrigation experiment at Wellington Caves (semi-arid, SE Australia), where cave dripwaters were shown to be a mix of tracer, modern and paleo-water (see Fig. 4 of [*Markowska et al.*, 2016]).

The two parameter Weibull distribution is represented as

$$f(x;\lambda,k) = \frac{k}{\lambda}\left(\frac{x}{\lambda}\right)^{k-1} e^{\left(-\frac{x}{\lambda}\right)^{k}}$$

where $x \geq 0, k > 0, \lambda > 0$.

The two parameters, k and λ, represent shape and scale, respectively (Fig. 2). The Weibull function is implemented over the domain $0 \leq x \leq 2$, divided over an adjustable-length mixing window. At each model step, k_diffuse determines the diffuse flow leaving the epikarst (see Table 2). This, along with the values for the previous months, is multiplied by the corresponding weights (y-values from Fig. 2) from the Weibull. The resulting flow entering KS1 (red arrow, Fig. 1) represents the diffuse flow amount for that month. Here, this process is applied to both water fluxes and mixing of $\delta^{18}O$ values, rather than just $\delta^{18}O$, as in Treble et al. (2013). It is implemented in the same manner every iteration (i.e. there are no seasonal factors included in the diffuse flow).

As shown in Fig. 2, the Weibull parameters, *k* and λ, control the residence time distribution. The scale parameter, *k*, controls where the peak occurs whereas the shape parameter, λ, can be used to change the distribution from left-skewed to right-skewed. As well as introducing a lag into the system, the diffuse flow parameterisation dampens the seasonal cycle. It does this more as the width of the peak increases, as shown in Fig. 2.

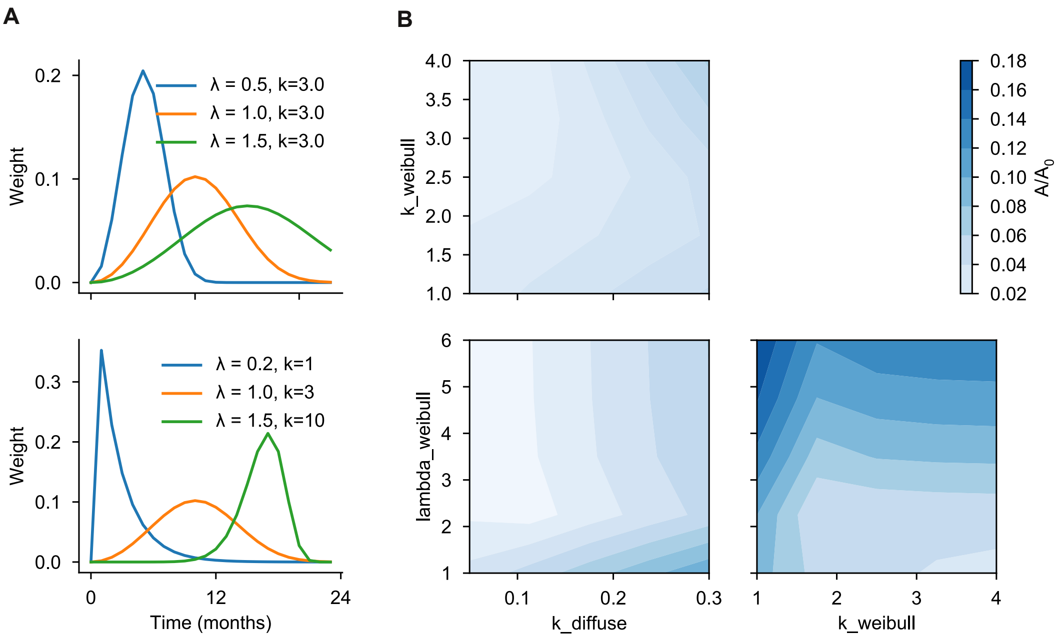

Figure 2. (a) Weibull distribution with parameters adjusted to change the peak width and shape. (b) the effect of changing the diffuse flow parameterisation on the amplitude, A, of a sinusoidal $\delta^{18}O$ input series. The input

$\delta^{18}O$ series has a period of 12 months, amplitude of A_0, monthly precipitation is held fixed, and other model parameters are set to the configuration given in Table 2.

2.5 Growth rate

The seasonal variation in speleothem growth rate can be important when comparing field observations to model output because the mean observed $\delta^{18}O$ will be weighted towards periods of faster growth. Speleothem growth rates are computed by Karstolution using the method presented by Kaufmann (2008), based on Dreybrodt (1999), whereby the growth rate, W_0, is

$$W_0 = 1.174\times10^3 \left(c - c_{app}\right) \frac{\delta}{\Delta d}\left[1 - \exp\left(-\frac{\alpha}{\delta}\Delta d\right)\right]$$

where c is the pCO_2 of water droplets, c_{app} is the apparent equilibrium pCO_2 of cave air ($1/\sqrt{0.8}$ times the cave air pCO_2), δ is the water film thickness (set to 0.01 cm), Δd is the drop interval, α is a rate constant, and the numerical factor is chosen so that W_0 has units of m year^{-1}. As with the calculation of $\delta^{18}O$, there is an optional correction for drop splashing (detailed by *Deininger et al.*, 2012).

3 Site description

Golgotha Cave, SW Western Australia (34°05'S, 115°03'E, Fig. 3), is located in a highly porous Quaternary-age calcarenite of aeolian origin. The present-day climate is Mediterranean-type. The cave is located at approximately 40 m depth under a wet eucalypt, evergreen forest (mixed *E. diversicolor and E. calophylla*). Drip monitoring studies at Golgotha Cave have shown consistent drip-rates despite the distinctly seasonal rainfall [*Treble et al.*, 2013]. LiDAR analysis coupled with high temporal and spatial-resolution drip-logger studies confirmed the dominance of diffuse flow, temporally consistent drip-rates and storage [*Mahmud et al.*, 2015; 2016; 2018]. For further details about Golgotha Cave studies refer to *Treble et al.* [2013], *Treble et al.* [2016], *Mahmud et al.* [2015] and *Mahmud et al.* [2016].

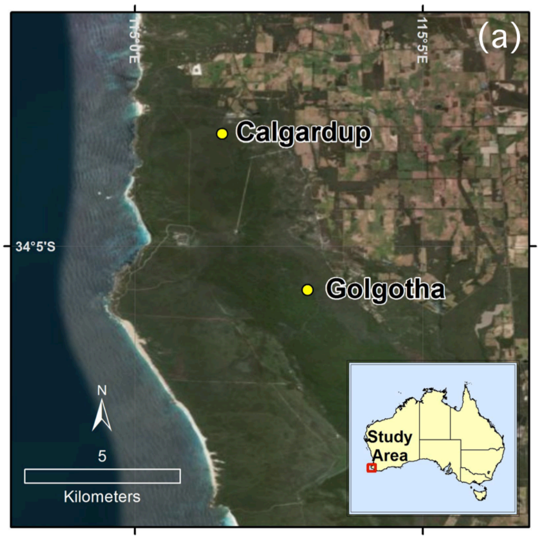

Figure 3. Location of Golgotha Cave in south-west Western Australia; the location of Calgardup Cave, where rainfall samples were collected, is also shown. The reader is referred to Figure 3 in Mahmud et al. [2016] for detailed site descriptions and maps.

4 Methods

4.1 Cave monitoring data

This study utilises data from August 2005 until March 2012 from Golgotha Cave that were previously published in Treble et al. (2013). Procedures for rainwater and dripwater sampling and analytical methods are presented in *Treble et al.* [2013; 2015].

The average cave parameters for each month of the year were determined by calculating the monthly means of the following data originally acquired at 15 min intervals using a Datataker DT80 logger between May 2017 and April 2018:

- relative humidity with a Vaisala HMP155 with Humicap 180RC and sensor warming enabled to negate saturation of the sensor at high humidity (accuracy ±1.8%);
- cave temperature with a Vaisala independent temperature probe (accuracy ±0.13°C);
- cave ventilation with a Gill Windsonic (±2%); and
- cave air pCO_2 with a Viasala GMP252 with measurement range 0-10,000 ppm (accuracy ±100 ppm). The longer cave air pCO_2 dataset (March 2009 – June 2014) presented in Treble et al. (2015) was used to match the time period of drip pCO_2 data (Treble et al., 2015).

4.2 Modern stalagmite $\delta^{18}O$ values

To further validate the model, modern stalagmite $\delta^{18}O$ data from the drip sites were compared with the model output. The method of sampling the modern calcite $\delta^{18}O$ is described in *Treble et al.* [2005]. Average stalagmite $\delta^{18}O$ values of approximately 10 years of growth preceding stalagmite sampling, and the range of values at each site and analytical error (0.07‰, 2 σ) was applied to quantify the uncertainties.

5 Results

5.1.1 In-cave processes

The monthly means from cave monitoring data used in the model are presented in Figs. 4a-c. Cave temperature displays a smooth seasonal cycle, peaking in February-April but with low overall variability (14.5-14.8°C; Fig. 4a). Other cave variables display similar seasonal maxima, also occurring in late summer/early autumn. Relative humidity is high (98 -100%; Fig. 4a). Cave-air and dripwater pCO_2 (Fig. 4b-c) demonstrate strong seasonality, reaching summer peaks of 2600 and 6800 ppmV and winter minimums of 540 and 1000 ppmV, respectively. This and the subtler seasonal trend in relative humidity are driven by temperature-driven gradients in seasonal cave ventilation (Treble et al., 2015) although air speed measurements demonstrate that air movement in the cave is low ($\leq$0.03 m s^{-1}; Fig. 4b).

5.1.2 Stalagmite calcite $\delta^{18}O$ values

Stalagmite $\delta^{18}O$ values are compared to the simulated Karstolution output as well as the output resulting from applying the equilibrium stable isotope fractionation factor of *Kim and O'Neil* [1997] (Fig. 5). Since Karstolution accounts for in-cave evaporative and disequilibrium isotope fractionation effects in addition to the equilibrium fractionation effect generated by the *Kim and O'Neil* [1997] equation, comparing the two outputs enables us to quantify the impact of in-cave disequilibrium fractionation. In general there is good agreement between the observed stalagmite $\delta^{18}O$ mean values and modelled outputs for Site 1A (Fig. 5) indicating that this stalagmite is precipitating at near isotopic equilibrium. The seasonal maxima of the Karstolution outputs overlap with the observed stalagmite means. This is consistent with the expectation that stalagmite deposition in Golgotha Cave will be biased towards the cooler months (Treble et al., 2015) and indicates that non-equilibrium processes may be more enhanced when the cave is in ventilated mode.

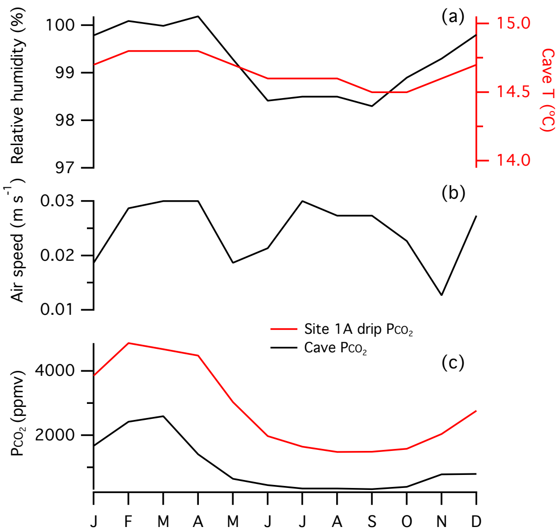

Figure 4: (a) Average monthly values for relative humidity and cave temperature. (b) Average monthly values for air speed. (c) Cave *p*CO_2 and calculated dripwater *p*CO_2 values. Calculated dripwater *p*CO_2 values are the dripwater *p*CO_2 values restored to calcite saturation (see Treble et al., 2015).

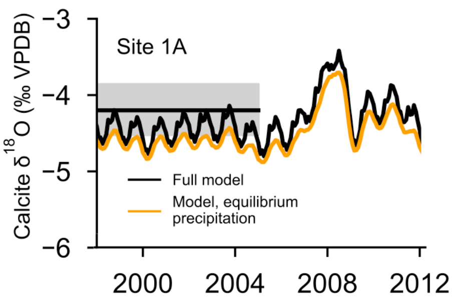

Figure 5. Comparison of observed stalagmite δ^{18}O values (grey bars) with modelled stalagmite δ^{18}O (orange: modelled dripwater δ^{18}O output converted to calcite assuming equilibrium oxygen isotope fractionation; black: full Karstolution output with ISOLUTION model enabled).

A sensitivity analysis was performed to determine which cave parameters potentially drive stalagmite δ^{18}O variability at Golgotha Cave. Figure 6 shows a reference case based on Site 1A, along with perturbations to cave parameters (Fig. 4). It demonstrated that the isotopic impact of temperature should be considered once mean cave temperature variability exceeds ±2°C (i.e., greater than that expected for the Holocene).

In terms of the potential isotopic impact of disequilibrium processes, stalagmite δ^{18}O appears to have some sensitivity to drip interval over the observed range for Golgotha Cave (Fig. 6b). The degree of disequilibrium increases at longer drip intervals as indicated by the departure from the predicted equilibrium δ^{18}O values. This is consistent with the expectation that deviation from isotopic equilibrium increases with the degree of calcite precipitation (Mühlinghaus et al., 2009; Deininger et al., 2012) before another drip falls. The sensitivity to changes in relative humidity and cave air movement are negligible due to the low variability of these parameters at Golgotha Cave (Fig. 6). The latter is in agreement with findings of negligible disequilibrium isotopic fractionation effects provided cave ventilation is less than 0.2 m/s and relative humidity greater than 85% [*Deininger et al.*, 2012; *Dreybrodt and Deininger*, 2014], and indicates that in-cave evaporative fractionation is not a driver of stalagmite δ^{18}O variability in this karst setting. Finally, the sensitivity of stalagmite δ^{18}O at Site 1A to the gradient between dripwater and cave pCO_2 is small to negligible (Fig. 6d), although this effect may become more important if the drip interval at this site were to increase (Fig. 6b).

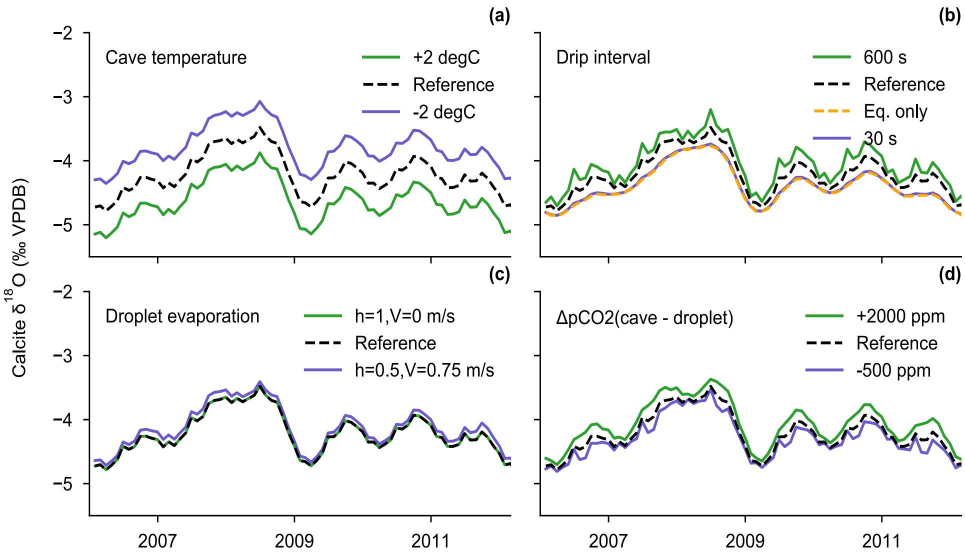

Figure 6. Sensitivity analysis for cave parameters at drip Site 1A: (a) cave temperature. (b) drip interval (c) relative humidity and cave ventilation. (d) cave air minus dripwater pCO_2. In order to preserve the measured seasonality in cave parameters, the reference case uses monthly values from Fig. 4 and perturbations have a constant offset across all months, with the addition of a limit to physically-realistic values (e.g. humidity must lie in the range 0-1). The predicted equilibrium calcite $\delta^{18}O$ from Figure 5 is also reproduced on Figure 6b for comparison.

6 Discussion

The cave-parameter sensitivity analysis (Fig. 6) demonstrated sensitivity of Golgotha Cave stalagmite $\delta^{18}O$ to cave temperature and drip interval and minimal isotopic effects of changes in evaporation and the cave air and dripwater pCO_2 gradient. Modelling the effects of in-cave disequilibrium isotope and evaporative fractionation over that of equilibrium isotope fractionation (Fig. 5) shows that at Golgotha Cave disequilibrium effects contribute negligibly to stalagmite $\delta^{18}O$ variability (Fig. 5). It is emphasised here that disequilibrium is accounted for in Karstolution, whereas kinetic fractionation is not. Disequilibrium isotope fractionation modelled by Karstolution accounts for the disturbance of the isotope equilibrium between $CaCO_3$, HCO_3^- and H_2O. In contrast, kinetic isotope fractionation represents the change of the isotope fractionation factor in relation to e.g., the precipitation rate (see Dietzl et al. 2009). Thus kinetic fractionation could be viewed as the offset between the Karstolution modelled values and the observed speleothem $\delta^{18}O$, implying that kinetic fractionation effects also have small to negligible isotopic impact on Golgotha Cave stalagmites. Adopting other fractionation factors (e.g. Coplen, 2007) may result in larger offsets compared to the predicted equilibrium output and may be appropriate for other locations.

One of the major advantages of Karstolution compared to previous stalagmite $\delta^{18}O$ PSMs is the isolation of various factors affecting isotopic values. For example, in analysing a Scottish millennial-length stalagmite with KarstFor, *Baker et al.* [2012] noted there was uncertainty if in-cave fractionation effects occur. In addition, integration of temperature-dependence of precipitation kinetics during calcite deposition, allows better representation and analysis of the effects of temperature and climate variability on stalagmite $\delta^{18}O$ values. This enables novel studies about both karst and cave effects, such as simulations of glacial-interglacial transitions, investigation of evaporative cooling [*Cuthbert et al.*, 2014b; *Rau et al.*, 2015] and the simulation of fire impacts, which increase soil evaporation and decrease the calcium content of the dripwater [*Nagra et al.*, 2016]. The ability to competently model these processes is critical in stalagmite $\delta^{18}O$ PSMs, augmenting the ability of these records to provide accurate quantifications of uncertainty in climate models.

7 Conclusions

This study represents the first integrated stalagmite $\delta^{18}O$ PSM: representing both karst hydrological and in-cave isotope fractionation processes. The primary assumptions incorporated into Karstolution have been conditionally confirmed based on its ability to generally simulate measured drip rate response and measured stalagmite $\delta^{18}O$ values, At Golgotha Cave, it is concluded that stalagmite $\delta^{18}O$ variability in the model is primarily driven by climatic inputs and the karst system rather than in-cave processes.

Future research will include model confirmation of Karstolution at other sites of different climates and hydrogeologies world-wide. Further modelling of the impacts of fire are also warranted. Future combination of Karstolution with GCMs and large climate models could also allow analysis of long-term model performance and facilitate realistic estimates of the variability of $\delta^{18}O$ values from the surface to the stalagmite.

Acknowledgments

We would like to thank Martin Andersen and Sylvia Dee for their comments on an earlier draft of the manuscript. We gratefully acknowledge the contributions of Nerilie Abram and Michael Gagan for laboratory analysis of speleothem $\delta^{18}O$ data and Petra Bajo and John Hellstrom for U-series chronology data that were utilised to calculate mean speleothem $\delta^{18}O$ values reported here. We also thank Barbora Gallagher for water isotope analyses, the Calgardup Caves staff (Department of Parks and Wildlife) for assisting with the cave monitoring data utilised here and Stuart Hankin for technical assistance in acquiring these data and drafting Fig. 3. This study contributes to ARC Discovery Project DP140102059 awarded to PCT and to ARC Linkage Project LP130100177 awarded to AB and PCT. MM was supported by DAAD funding. MD and DS acknowledges funding of the DFG through grants DE 2398/3-1 and SCHO 1274/9-1, respectively..

References

Affek, H. P., M. Bar-Matthews, A. Ayalon, A. Matthews, and J. M. Eiler (2008), Glacial/interglacial temperature variations in Soreq cave speleothems as recorded by 'clumped isotope' thermometry, *Geochimica et Cosmochimica Acta*, *72*(22), 5351-5360.

Ayalon, A., M. Bar-Matthews, and E. Sass (1998), Rainfall-recharge relationships within a karstic terrain in the Eastern Mediterranean semi-arid region, Israel: $\delta^{18}O$ and δD characteristics, *Journal of Hydrology*, *207*(1), 18-31.

Baker, A., and C. Brunsdon (2003), Non-linearities in dripwater hydrology: an example from Stump Cross Caverns, Yorkshire, *Journal of Hydrology*, *277*(3-4), 151-163.

Baker, A., and C. Bradley (2010), Modern stalagmite $\delta^{18}O$: Instrumental calibration and forward modelling, *Global and Planetary Change*, *71*(3-4), 201-206.

Baker, A., C. Bradley, and S. J. Phipps (2013), Hydrological modeling of stalagmite $\delta^{18}O$ response to glacial-interglacial transitions, *Geophysical Research Letters*, *40*(12), 3207-3212.

Baker, A., C. Bradley, S. J. Phipps, M. Fischer, I. J. Fairchild, L. Fuller, C. Spötl, and C. Azcurra (2012), Millennial-length forward models and pseudoproxies of stalagmite δ18O: an example from NW Scotland, *Climate of the Past*, *8*(4), 1153-1167.

Baker, A., A. Asrat, I. J. Fairchild, M. J. Leng, L. Thomas, M. Widmann, C. N. Jex, Buwen Dong, P. van Calsteren, and C. Bryant (2010), Decadal-scale rainfall variability in Ethiopia recorded in an annually laminated, Holocene-age, stalagmite, *The Holocene*, *20*(6), 827-836.

Baker, A. J., D. P. Mattey, and J. U. L. Baldini (2014), Reconstructing modern stalagmite growth from cave monitoring, local meteorology, and experimental measurements of dripwater films, *Earth and Planetary Science Letters*, *392*, 239-249.

Baldini, J. U. L., F. McDermott, L. M. Baldini, C. J. Ottley, K. L. Linge, N. Clipson, and K. E. Jarvis (2012), Identifying short-term and seasonal trends in cave dripwater trace element concentrations based on a daily-scale automatically collected dripwater dataset, *Chemical Geology*, *330-331*, 1-16.

Bradley, C., A. Baker, C. N. Jex, and M. J. Leng (2010), Hydrological uncertainties in the modelling of cave drip-water $\delta^{18}O$ and the implications for stalagmite palaeoclimate reconstructions, *Quaternary Science Reviews*, *29*(17-18), 2201-2214.

Coplen, T.B. (2007), Calibration of the calcite-water oxygen-isotope geothermometer at Devils Hole, Nevada, a natural laboratory. *Geochimica et Cosmochimica Acta* 71, 3948-3957.

Cuthbert, M. O., A. Baker, C. N. Jex, P. W. Graham, P. C. Treble, M. S. Andersen, and I. R. Acworth (2014a), Dripwater isotopes in semi-arid karst: Implications for speleothem paleoclimatology, *Earth and Planetary Science Letters*, *395*, 194-204.

Cuthbert, M. O., et al. (2014b), Evaporative cooling of speleothem dripwater, *Scientific reports*, *4*, 5162.

Dee, S. G., N. J. Steiger, J. Emile-Geay, and G. J. Hakim (2016), On the utility of proxy system models for estimating climate states over the common era, *Journal of Advances in Modeling Earth Systems*, *8*(3), 1164-1179.

Deininger, M., & Scholz, D. (2019). ISOLUTION 1.0: an ISOtope evoLUTION model describing the stable oxygen (δ18O) and carbon (δ13C) isotope values of speleothems. *International Journal of Speleology, 48*, 3. doi:https://doi.org/10.5038/1827-806X.48.1.2219

Deininger, M., J. Fohlmeister, D. Scholz, and A. Mangini (2012), Isotope disequilibrium effects: The influence of evaporation and ventilation effects on the carbon and oxygen isotope composition of speleothems – A model approach, *Geochimica et Cosmochimica Acta*, *96*, 57-79.

Dietzel, M., J. Tang, A. Leis, and S. J. Köhler (2009), Oxygen isotopic fractionation during inorganic calcite precipitation — Effects of temperature, precipitation rate and pH, *Chemical Geology, 268,* 107-115.

Dorale, J. A., and Z. Liu (2009), Limitations of hendy test criteria in judging the paleoclimatic suitability of speleothems and the need for replication, *Journal of Cave and Karst Studies*, *71*(1), 73-80.

Dreybrodt, W., and M. Deininger (2014), The impact of evaporation to the isotope composition of DIC in calcite precipitating water films in equilibrium and kinetic fractionation models, *Geochimica et Cosmochimica Acta*, *125*, 433-439.

Duan, W. H., J. Y. Ruan, W. J. Luo, T. Y. Li, L. J. Tian, G. N. Zeng, D. Z. Zhang, Y. J. Bai, J. L. Li, T. Tao, P. Z. Zhang, A. Baker and M. Tan (2016), The transfer of seasonal isotopic variability between precipitation and dripwater at eight caves in the monsoon regions of China, *Geochimica et Cosmochimica Acta*, *183*, 250-266.

Evans, M. N., S. E. Tolwinski-Ward, D. M. Thompson, and K. J. Anchukaitis (2013), Applications of proxy system modeling in high resolution paleoclimatology, *Quaternary Science Reviews*, *76*, 16-28.

Fairchild, I. J., G. W. Tuckwell, A. Baker, and A. F. Tooth (2006), Modelling of dripwater hydrology and hydrogeochemistry in a weakly karstified aquifer (Bath, UK): Implications for climate change studies, *Journal of Hydrology*, *321*(1-4), 213-231.

Frisia, S., I. J. Fairchild, J. Fohlmeister, R. Miorandi, C. Spötl, and A. Borsato (2011), Carbon mass-balance modelling and carbon isotope exchange processes in dynamic caves, *Geochimica et Cosmochimica Acta*, *75*(2), 380-400.

Hartmann, A. and A. Baker (2017), Modelling karst vadose zone hydrology and its relevance for paleoclimate reconstruction, Earth Science Reviews, 172, 178-192.

Hendy, C. H. (1971), The isotopic geochemistry of speleothems—I. The calculation of the effects of different modes of formation on the isotopic composition of speleothems and their applicability as palaeoclimatic indicators, *Geochimica et Cosmochimica Acta*, *35*(8), 801-824.

Jones, D. A., W. Wang, and R. Fawcett (2009), High-quality spatial climate data-sets for Australia." Australian Meteorological and Oceanographic Journal 58(4), 233.

Kaufmann, G. (2003), Stalagmite growth and palaeo-climate: the numerical perspective, *Earth and Planetary Science Letters*, *214*(1-2), 251-266.

Kim, S.-T., and J. R. O'Neil (1997), Equilibrium and nonequilibrium oxygen isotope effects in synthetic carbonates, *Geochimica et Cosmochimica Acta*, *61*(16), 3461-3475.

Kluge, T., T. Marx, D. Scholz, S. Niggemann, A. Mangini, and W. Aeschbach-Hertig (2008), A new tool for palaeoclimate reconstruction: Noble gas temperatures from fluid inclusions in speleothems, *Earth and Planetary Science Letters*, *269*(3–4), 408-415.

Mahmud, K., G. Mariethoz, P. C. Treble, and A. Baker (2015), Terrestrial LiDAR Survey and Morphological Analysis to Identify Infiltration Properties in the Tamala Limestone, Western Australia, *IEEE Journal of Selected Topics in Applied Earth Observations and Remote Sensing*, *8*(10), 4871-4881. doi: 10.1109/JSTARS.2015.2451088

Mahmud, K., G. Mariethoz, A. Baker, P. C. Treble, M. Markowska, and E. McGuire (2016), Estimation of deep infiltration in unsaturated limestone environments using cave lidar and drip count data, *Hydrol. Earth Syst. Sci.*, *20*(1), 359-373. doi:10.5194/hess-20-359-2016

Mahmud, K., G. Mariethoz, A. Baker, and P.C. Treble, P.C. (2018), Hydrological characterization of cave drip waters in a porous limestone: Golgotha Cave, Western Australia, *Hydrological and Earth System Sciences 22*, 977-988. https://doi.org/10.5194/hess-22-977-2018

Markowska, M., A. Baker, P. C. Treble, M. S. Andersen, S. I. Hankin, C. N. Jex, C. V. Tadros, and R. Roach (2015), Unsaturated zone hydrology and cave drip discharge water response: Implications for speleothem paleoclimate record variability, *Journal of Hydrology*, *529*, 662-675.

McDermott, F. (2004), Palaeo-climate reconstruction from stable isotope variations in speleothems: a review, *Quaternary Science Reviews*, *23*(7-8), 901-918.

Mickler, P. J., L. A. Stern, and J. L. Banner (2006), Large kinetic isotope effects in modern speleothems, *Geological Society of America Bulletin*, *118*(1-2), 65-81.

Mischel, S., D. Scholz, and C. Spötl (2015), $\delta^{18}O$ values of cave dripwater: a promising proxy for the reconstruction of the North Atlantic Oscillation?, *Clim Dyn*, 1-16.

Mühlinghaus, C., Scholz, D. and Mangini, A. (2007), Modelling stalagmite growth and $\delta^{13}C$ as a function of drip interval and temperature, *Geochimica et Cosmochimica Acta* 71, 2780-2790.

Mühlinghaus, C., D. Scholz, and A. Mangini (2009), Modelling fractionation of stable isotopes in stalagmites, *Geochimica et Cosmochimica Acta*, *73*(24), 7275-7289.

Nagra, G., P. C. Treble, M. S. Andersen, I. J. Fairchild, K. Coleborn, and A. Baker (2016), A post-wildfire response in cave dripwater chemistry, *Hydrology and Earth System Sciences, 20(7), 2745-2758.*

Pape, J. R., J. L. Banner, L. E. Mack, M. Musgrove, and A. Guilfoyle (2010), Controls on oxygen isotope variability in precipitation and cave dripwaters, central Texas, USA, *Journal of Hydrology*, *385*(1-4), 203-215.

Rau, G. C., M. O. Cuthbert, M. S. Andersen, A. Baker, H. Rutlidge, M. Markowska, H. Roshan, C. E. Marjo, P. W. Graham, and R. I. Acworth (2015), Controls on cave dripwater temperature and implications for speleothem-based paleoclimate reconstructions, *Quaternary Science Reviews*.

Riechelmann, D.F.C., Deininger, M., Scholz, D., Riechelmann, S., Schröder-Ritzrau, A., Spötl, C., Richter, D.K., Mangini, A. and Immenhauser, A. (2013), Disequilibrium carbon and oxygen isotope fractionation in recent cave calcite: Comparison of cave precipitates and model data, *Geochimica et Cosmochimica Acta* 103, 232-244.

Scholz, D., C. Mühlinghaus, and A. Mangini (2009), Modelling $\delta^{13}C$ and $\delta^{18}O$ in the solution layer on stalagmite surfaces, *Geochimica et Cosmochimica Acta*, *73*(9), 2592-2602.

Spötl, C., I. J. Fairchild, and A. F. Tooth (2005), Cave air control on dripwater geochemistry, Obir Caves (Austria): Implications for speleothem deposition in dynamically ventilated caves, *Geochimica et Cosmochimica Acta*, *69*(10), 2451-2468.

Stoll, H. M., A. Mendez-Vicente, S. Gonzalez-Lemos, A. Moreno, I. Cacho, H. Cheng, and R. L. Edwards (2015), Interpretation of orbital scale variability in mid-latitude speleothem $\delta^{18}O$: Significance of growth rate controlled kinetic fractionation effects, *Quaternary Science Reviews*.

Treble, P. C., J. Chappell, M. Gagan, K. McKeegan, and T. Harrison (2005), In situ measurement of seasonal $\delta^{18}O$ variations and analysis of isotopic trends in a modern speleothem from southwest Australia, *Earth and Planetary Science Letters*, *233*(1-2), 17-32.

Treble, P. C., C. Bradley, A. Wood, A. Baker, C. N. Jex, I. J. Fairchild, M. K. Gagan, J. Cowley, and C. Azcurra (2013), An isotopic and modelling study of flow paths and storage in Quaternary calcarenite, SW Australia: implications for speleothem paleoclimate records, *Quaternary Science Reviews*, *64*, 90-103.

Treble, P. C., I. J. Fairchild, A. Griffiths, A. Baker, K. T. Meredith, A. Wood, and E. McGuire (2015), Impacts of cave air ventilation and in-cave prior calcite precipitation on Golgotha Cave dripwater chemistry, southwest Australia, *Quaternary Science Reviews*.

Treble, P. C., I. J. Fairchild, A. Baker, K. T. Meredith, M. S. Andersen, S. U. Salmon, C. Bradley, P. M. Wynn, S. Hankin, A. Wood and E. McGuire (2016), Roles of forest bioproductivity, transpiration and fire in a nine-year record of cave dripwater chemistry from southwest Australia, *Geochimica et Cosmochimica Acta*, *184*, 132-150.

Wong, C. I., and D. O. Breecker (2015), Advancements in the use of speleothems as climate archives, *Quaternary Science Reviews*, *127*, 1-18.